AI Analysis Basic Course
First Installment: Neural Network Application to Phase Identification in Powder X-ray Diffraction

Toshihide Shibasaki*, Takumi Ohta** and Akihiro Himeda*

Abstract

In recent years, there have been significant improvements in AI technology, especially in neural networks. We describe profile-based phase identification using neural networks, which does not require peak search. Using cements and excipients as examples, we report that neural networks can be used to identify crystalline phases more accurately even when analysis by the conventional method is difficult.

1. Introduction

Phase identification is one of the basic analyses of powder X-ray diffraction (powder XRD). Although X-ray diffraction software such as SmartLab Studio II[(1)] automates the procedure to list phase candidates from XRD profiles, inspection by experts is required to finally determine the crystalline phases. To make this analysis easier, it is important to have a method to obtain more accurate phase candidates.

Conventionally, peak-based methods have been widely used for phase identification in powder XRD, including the Hanawalt method, which is a manual analysis method[(2)]. In peak-based methods, peak search is first performed on the XRD profiles to make a list of peak positions and intensities (d–I list). This d–I list is then compared with the diffraction patterns of known materials to obtain phase candidates. However, in profiles with many overlapping peaks or broad peaks due to poor crystallinity, it is difficult to perform peak search accurately and sometimes the correct candidates cannot be obtained.

Recently, a phase identification method using neural networks has been proposed[(3)]. Neural networks are AI models that imitate the network structure of cranial nerves. They can be trained by inputting training data to solve tasks such as image classification, for example. The technology of neural networks has been improving dramatically, with many models appearing that can perform very complex tasks, such as large language models*1. Neural networks can be used to perform profile-based phase identification without peak search. Therefore, it is expected that more accurate phase candidates can be obtained for profiles that are difficult to analyze by conventional methods.

In this paper, we describe the method of phase identification using neural networks. Using cements

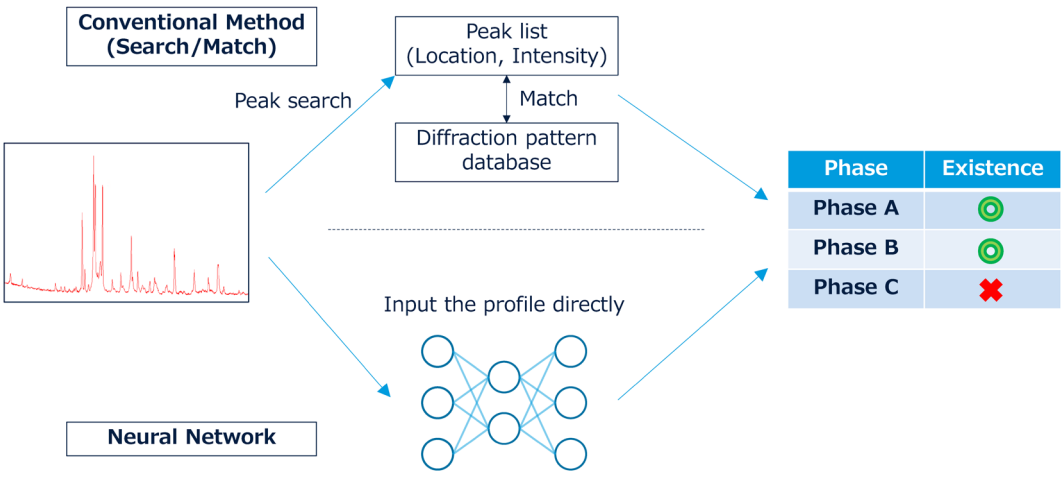

Fig. 1. Comparison of the procedures of phase identification by the conventional method (search/match) and neural networks.

* XRD Application & Software Development, Product Division, Rigaku Corporation.
** X-ray Research Laboratory, Rigaku Corporation.

*1 Large AI models which specialize in language understanding and generation such as ChatGPT (invented by OpenAI).

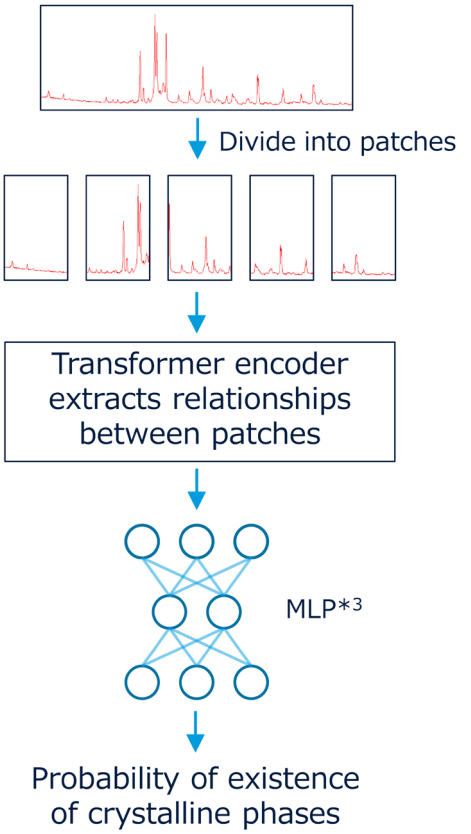

Fig. 2. Phase identification by the vision transformer.

and pharmaceutical excipients*2 as examples, which are typical materials difficult to analyze by conventional methods, we report that the use of neural networks enabled more accurate analysis.

2. Phase Identification by Neural Networks

In Fig. 1, the procedures of phase identification by the conventional search/match method and by neural networks are compared. As mentioned above, in search/match, a peak-based method, phase identification is performed by first making a peak list from the XRD profile and then matching it with the diffraction pattern database. On the other hand, in phase identification by neural networks, the measured XRD profile (or a pre-processed profile, such as one where the background has been subtracted) is directly input to a neural network to perform phase identification. Therefore, the results by neural networks are essentially independent of the peak search accuracy.

In this study, we used a vision transformer (ViT)[4] as a neural network model for phase identification, which is known as a high-performance image recognition model. The process flow of phase identification by a ViT is shown in Fig. 2. ViTs have a structure called a transformer*4 by which an input image is divided into multiple patches and the relationships between them

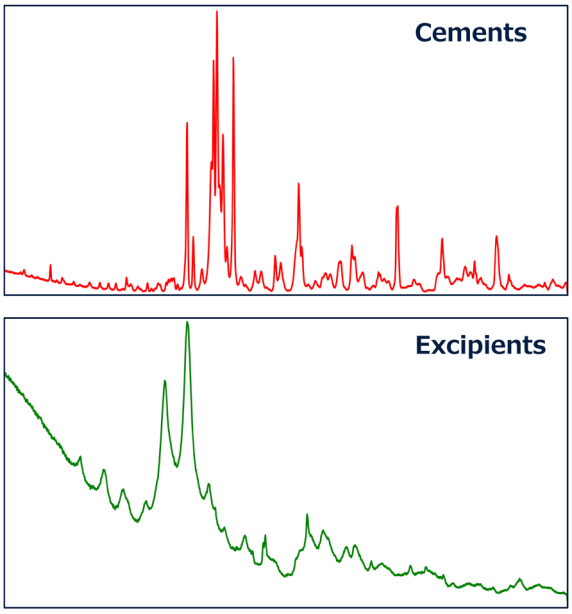

Fig. 3. Examples of XRD profiles of cements and excipients.

are evaluated to recognize spatially separated features on the image[5]. In our case, the input image is a one-dimensional XRD profile. It is expected that the ViT associates discrete features such as peaks to identify the crystalline phases.

3. Evaluation method

3.1. Data preparation

We chose cements and pharmaceutical excipients as materials to compare phase identification by search/match and by neural networks. Examples of XRD profiles of cements and excipients are shown in Fig. 3. It is difficult to identify phases in cements by search/match because there are many overlapping peaks due to the multiple polymorphs with similar diffraction patterns in their major components*5. Likewise, phase identification by search/match is also difficult for excipients because they generally contain micro-crystals and amorphous components and thus have broad peaks.

We prepared a small database for each of these two materials to perform phase identification for them. The cements database contained 72 phase entries, of which 28 were major components (C3S: 7 entries, C2S: 12 entries, C3A: 6 entries, C4AF: 3 entries) and 44 entries were other minor components contained in usual cements. The excipients database consisted of 40 phase entries, of which 8 were crystals, 24 were micro-crystals and 8 were amorphous phases.

Next, we describe the training data for the neural networks. We used simulated profiles generated by the

*2 Inactive substances used in the formulation of drugs.
*3 Multi-Layer Perceptron. Simple neural networks with several fully connected layers.
*4 The transformer technique was originally developed in language models and used in current large language models. ViTs have achieved great success when applied to image recognition.
*5 Cements generally contain alite (C3S), belite (C2S), aluminate (C3A) and ferrite (C4AF) as major components. There are several polymorphs and phases with slightly different compositions for these components.

fundamental parameter (FP) method*6 in SmartLab Studio II as training data. The following strategy proposed in the previous study(3) was adopted as a method to generate large amounts of data in a short time.

(1) Simulated single phase profiles of each crystalline phase in the databases by the FP method. Here, several patterns of profiles were generated by varying the phase parameters (lattice constants, crystallite size and preferred orientation). This was to include differences of profile shapes due to phase parameters in the training data.
(2) Added the simulated single phase profiles together at random to generate mixture profiles.

The mixture profiles generated in this way were the input to the neural networks. The neural networks output the certainty of inclusion of each crystalline phase (as a continuous value between 0 and 1) and were optimized (trained) to output 1 for the included phases and 0 for the not-included phases.

Then, we describe the test data used for the evaluation. As common test data for search/match and neural networks, 1000 mixture profiles were generated for each of cements and excipients by the FP method. For cements, all data contained one phase from each of the four major components (C3S, C2S, C3A and C4AF) and one or two minor phases. The minimum weight fraction was 1 wt% for each minor phase. On the other hand, for excipients, all data contained a random selection of two to eight phases, with a minimum weight fraction of 2 wt% for each phase. Crystallite sizes were 60–140 nm for crystals, 10–20 nm for micro-crystals and 1–2 nm for amorphous phases.

3.2. Phase identification procedures

In the evaluation, we performed phase identification by search/match using the following procedure*7:

(1) Executed peak search and fit profiles with split pseudo-Voigt functions for peaks and a B-spline function for background.
(2) Performed phase identification by matching with the database.

Phase identification by neural networks was performed in the following procedure:

(1) Subtracted background by fitting with a polynomial function.
(2) Input the background subtracted profile to the trained neural network. The neural network output the certainty of inclusion of each phase. If the value was greater than or equal to 0.5, it was judged as included, otherwise it was judged as not included.

3.3. Indicators

We used three indicators called recall, accuracy and F1 values to compare the results by search/match and by neural networks. These are defined as follows. Let the true positive rate be TP, the false positive rate be FP and the false negative rate be FN. Using these, the recall and the precision are defined by the following equations.

$$\text{Recall} = \text{TP}/(\text{TP}+\text{FN}) \tag{1}$$

$$\text{Precision} = \text{TP}/(\text{TP}+\text{FP}) \tag{2}$$

A higher recall means fewer missed detections of the phases, and a higher precision means fewer false detections. Using the recall and the precision, the F1 value is given by the following equation.

$$\text{F1} = 2 \times \frac{\text{Recall} \times \text{Precision}}{\text{Recall} + \text{Precision}} \tag{3}$$

The closer the F1 value is to 1, the higher both the recall and the precision, meaning that the phase identification results are more accurate. The neural networks were trained three times for each material and the average scores are shown in this paper.

4. Results

4.1. Cements

Table 1 shows the results of phase identification for the cements test data. The neural network scores were significantly higher than the search/match scores, indicating that phase identification was performed more accurately including polymorphs of the major components. The low recall for minor components by search/match means that trace components could not be detected in many cases.

For cements, in addition to the evaluation using the simulation data, we also carried out evaluation using the measured profile of the NIST 2686 clinker*8 standard sample. This was performed according to the following procedure:

(1) Executed phase identification for the measured data of the NIST 2686 sample by search/match and neural networks.
(2) Performed Rietveld analysis using phases selected above and compared the weight fractions with the NIST certified values.

The result of this evaluation is shown in Table 2. Although the same phases were identified for most of the components by search/match and neural networks, different crystal systems were identified for C3S, one of the main components. This caused large differences in the quantitative values by Rietveld analysis and the phase candidates by neural networks gave closer values to the certified values. This implies that the neural networks was able to select more appropriate phases and was superior in identifying polymorphs.

4.2. Excipients

The results for the excipients test data are shown in Table 3. The neural networks also outperformed search/match on most scores for excipients. The superiority

*6 The method to simulate diffraction patterns using the convolution of profile shape derived from crystallite size and lattice strain, profile shape derived from emission profile of incident X-ray and profile derived from each type of device.
*7 This is the default analysis procedure in SmartLab Studio II.
*8 Main raw material for cements.

Table 1. Phase identification results for the cements test data.

		Recall	Precision	F1
All phases	Neural networks	0.752	0.841	0.794
	Search/Match	0.448	0.621	0.520
Major phases	Neural networks	0.825	0.822	0.824
	Search/Match	0.516	0.633	0.568
Minor phases	Neural networks	0.591	0.944	0.727
	Search/Match	0.287	0.583	0.384

Table 2. Results of evaluation by the measured data of NIST 2686.

Phase	Neural networks		Search/Match		Certified values
	Crystal systems of identified phases	Weight fraction/wt%	Crystal systems of identified phases	Weigt fraction/wt%	Weight fraction/wt%
C3S	Monoclinic	57.5 (0.4)	Rhombohedral	44.5 (0.6)	58.6±4.0
C2S	Monoclinic	24.6 (0.4)	Monoclinic	35.1 (0.6)	23.3±2.8
C3A	Cubic	0.3 (0.3)	Cubic	0.2 (0.7)	2.3±2.1
C4AF	Orthorhombic	13.1 (0.3)	Orthorhombic	14.0 (0.4)	14.1±1.4
Periclase	—	4.41 (0.12)	—	6.10 (0.19)	3.3±1.9

Estimated standard deviations in brackets (1σ).

Table 3. Phase identification results for the excipients test data.

		Recall	Precision	F1
All phases	Neural networks	0.732	0.823	0.775
	Search/Match	0.501	0.848	0.630
Crystals	Neural networks	0.945	0.943	0.944
	Search/Match	0.834	0.962	0.894
Micro-crystals	Neural networks	0.759	0.918	0.831
	Search/Match	0.571	0.830	0.677
Amorphous	Neural networks	0.434	0.433	0.433
	Search/Match	0.043	0.338	0.076

of the neural networks was particularly remarkable for micro-crystals. Therefore, neural networks are more suitable for phase identification for samples with poor crystallinity. On the other hand, for identification of the amorphous phases, it is hard to say that the phases were identified sufficiently even by neural networks although their scores were higher than the search/match scores. It is believed that this is because the real background could not be separated from the amorphous profiles when subtracting background during pre-processing.

As an example of a practical use case, we therefore evaluated identification of crystals and micro-crystals, excluding amorphous phases which are difficult to identify by either method. In other words, amorphous phases were excluded from the excipients database and this database was used to train the neural networks. Amorphous phases were also excluded from the target database of search/match. However, the test data still contained amorphous components, and we investigated whether crystals and micro-crystals could be identified from them by search/match and neural networks. The procedure of phase identification by neural networks was modified as follows to perform this evaluation:

(1) Executed peak search to detect peaks of crystals and micro-crystals. Then, fit peaks and background to subtract background including the amorphous halos.
(2) Input the background subtracted profile to the trained neural network to identify phases.

Note that this method uses peak search for background subtraction, and therefore the results of phase identification by neural networks are also affected by peak search. However, the input to the neural networks is still a profile rather than a peak list. Thus, it is expected that even if overlapping peaks cannot be accurately separated, for example, the accuracy of phase identification is not as affected so long as the effect on fitting background is minor.

Table 4 shows the results of this evaluation. Although

Table 4. Phase identification results when amorphous phases are excluded.

		Recall	Precision	F1
Crystals	Neural networks	0.959	0.910	0.934
	Search/Match	0.838	0.941	0.887
Micro-crystals	Neural networks	0.825	0.762	0.792
	Search/Match	0.572	0.804	0.668

search/match slightly outperformed the neural networks in precision, the neural networks gave significantly higher recall values than search/match. The difference in recall for micro-crystals was particularly remarkable, indicating that the neural network had fewer missed detections of micro-crystals. Therefore, the combined use of peak search to subtract non-monotonic background is also practical for the detection of (micro-) crystals.

5. Summary

We have compared phase identification by the conventional search/match method and by neural networks. Search/match is a peak-based method and therefore sometimes does not identify the correct crystalline phases for profiles where accurate peak search is difficult. On the other hand, phase identification by neural networks is profile-based and basically independent of the accuracy of peak search. In this paper, we have evaluated the results of phase identification by these two methods for cements and pharmaceutical excipients. These materials are typical examples of those which are difficult to analyze by search/match since the cements profiles have many overlapping peaks and excipients profiles have broad peaks due to poor crystallinity. We have shown that the use of neural networks to identify phases gave more accurate results for these materials.

References

(1) *Rigaku Journal*, **31** (2015), No.2, 25–26.
(2) Rigaku Corporation: Handbook of X-ray Diffraction (7th edition).
(3) J. Schuetzke, A. Benedix, R. Mikut, and M. Reischl: *IUCrJ*, **8** (2021), 408–420.
(4) A. Dosovitskiy, L. Beyer, A. Kolesnikov, D. Weissenborn, X. Zhai, T. Unterthiner, M. Dehghani, M. Minderer, G. Heigold, S. Gelly, J. Uszkoreit, and N. Houlsby: Proceedings of the *International Conference on Learning Representations 2021*, (2021).
(5) A. Vaswani, N. Shazeer, N. Parmar, J. Uszkoreit, L. Jones, A. N. Gomez, L. Kaiser, and I. Polosukhin: Proceedings of the *31st International Conference on Neural Information Processing Systems*, (2017), 6000–6010.